IOP Conf. Series: Materials Science and Engineering **382** (2018) 052008 doi:10.1088/1757-899X/382/5/052008

The Numerical Investigation of Optical Error Compensation for Dynamic Target by FSM in Photoelectric Mast *

Zong Kai Liu*, Yu Ming Bo, Jun Wang, Ke Cui

Key Laboratory of Advanced Solid-State Laser, Nanjing University of Science and Technology, Nanjing, Jiangsu 210094, China

Email: kfliukai@126.com

Abstract: In this paper, firstly, based on the basic control equations of fluid mechanics, the effects of the fluid on force and vortex induced vibration around underwater submarine model are studied and discussed, employing the finite volume method by hierarchy grids. Secondly, the structural characteristics, transfer functions and control strategies of Steering Mirror Fast (FSM) are analyzed and obtained. The disturbance of moment also has been resolved to optical axis coordinate system. Finally, take the optical model of submarine as the research background, the effects of the FSM on the stability improvement of photoelectric tracking system are discussed. The results show that the disturbance of submarine moments mainly origin from the vortex induced vibration. The dynamic target tracking error could be suppressed. This research explores vortex induced vibration control in optical filter. Therefore, it holds certain scientific significance and practical value.

1. Introduction

The photoelectric mast offers several applications on target searching, laser ranging, laser communication, laser weapon as well as optical tracking[1][2]. For the submarine, the photoelectric and optical tracking system required to be installed into the long photoelectric masts. However, when submarines carrying long mast and traveling at high speed under water, several unnegligible disturbances would be generated, due to the interaction of the seawater. For larger Reynolds number environment (laminar flow), the seawater would be removed from the submarine' surface and form complex vortex street, which will cause large fluid dynamics fluctuation. Previous researchers[3][4] have done a lot of researches on underwater vehicles. They found that the yawing, pitching and rolling three disturbance trends of movement would be caused by the moments vehicles suffering, which could inevitably increase the angle tracking error of the submarine tracking-pointing device. Furthermore, the translational as well as the rotating motion of this submarine is caused by these force or moment. The characters of flow field structure, force and moment could be significant influenced by sailing posture, Reynolds number and so on. These disturbances, finally, would be added to the input noise of tracking and targeting systems in the apparent axis coordinate system. Previously, in the field of fluid mechanics, the studies of submarine flow field and vibration have been widely carried out. Those disturbances usually appear narrow bandwidth and small amplitude. In order to compensate the optical axis error caused by these disturbances, adaptive optics structure is applied on the tracking-pointing servo system. The FSM is an important optical equipment, by control two pairs of piezoelectric ceramics stack one pair push and the other pair pull with certain angles[5][6] the reflected light could be adjusted accurately and fastly.

In this paper, firstly, the character of force and fluid field for a submarine model at 6° yaw angle,

Reynolds number $Re=10^7$ has been numerical simulated. Secondly, the disturbance of force and moment has been carefully calculated and transferred into the azimuth and pitch angle in submarine polar coordinate system, respectively. Finally, the compensate error based on FSM transfer function and closed-loop control strategy have been analysis by MATLAB Simulink simulation. By discussing the simulation results as well as the force and flow field evolution, the interaction mechanism for submarine disturbance, flow field structure and the tracking accuracy are discussed.

2. Basic model and numerical method

As figure 1 show, the submarine is composed with hemispherical head, cylindrical body and conical tail, where the length for these parts is 0.06l, 0.69l, 0.25l, respectively. And l is the chord as well as the character length in this simulation. The other specific sizes for this model also displayed in figure 1.

The size of this computational domain is 4l×2l×2l, the inlet flow along the x-positive direction, the leading point of the submarine at the origin of right-handed coordinate system, and keeping 0.5l away from the inlet surface. The X-axis points to downstream, the Y-axis points to the starboard, and the Z-axis to the vertically upwards. In this simulation, for the computational domain, the left and right surface is define as speed entry and pressure outlet boundary conditions, respectively, the other four side surfaces are defined as pressure boundary condition, on which the pressure is constant and the velocity in normal direction is zero. Additional, the surface of submarine is defined as no slip boundary condition.

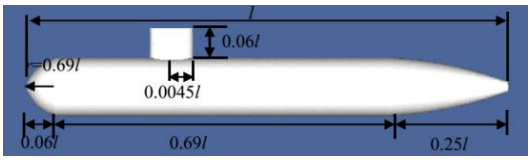

Figure 1 The structure of the submarine model

For spatial discretization, the computational area is divided into the several Quad-Tree (two dimensional) or Octree (three dimensional) structure cells[7][8]. The second-order upwind scheme of Bell-Colella-Glaz is applied on the discrete of convection terms, and this discrete scheme is stabilize for CFL<1. The diffusive term is discreted by Crank-Nicholson method, which has several advantages such as second order accuracy and unconditional stability. Above all, in this simulation, time and space dispersion have second order precision[9].

3. The influence of the submarine moment on the azimuth/pitch angle

The photoelectric tracking system loaded in the optronic mast would be influence by the fluid while it interacts with submarine. If the submarine is considered as unrestraint rigid body. It could move and roll freely at the 6 freedom degrees (translational motion 3, rotating motion 3). However, during the numerical simulation the attitudes of the submarine keep constant, so the motion has six kinds of motion trend, including rolling, pitching, yawing and surging，swaying, heaving. It could be considered that, for the shorter sampling period (0.01s~0.02s) of CCD, the influence of those moment disturbance could not make the target beyond the view field of the optical detector. And the photoelectric tracking system is fixed on the submarine optronic mast, so its movement will keep pace with the submarine. In the solution, the translation and rocking movement need to be treated by different formulas. Furthermore, based on the force and moment, the translational motion speed as well as rotation angle speed can be solved.

Compare with submarine swaying motion, the influence of submarine translational motion could be ignored for the short CCD sampling period (within 0.01s~0.02s). Thus, this paper only discusses the swaying motion influence for azimuth and pitch angles on optical axis coordinate system.

The angular displacement model of the optic axis disturbance: the attitude of the submarine at any point in the sea can be determined by the three attitude angles (yawing angler α_H, rolling angle α_P and pitching angle α_R) in submarine coordinate system or earth coordinate system. The azimuthal

angle and pitch angle in submarine coordinate (X_d, Y_d, Z_d) could be solved by α_H、α_p、α_R and Δt, independently, based on the target point coordinate $G(x,y,z)$ in earth coordinate system (X,Y,Z). The algorithm flow charts are presented in figure 2.

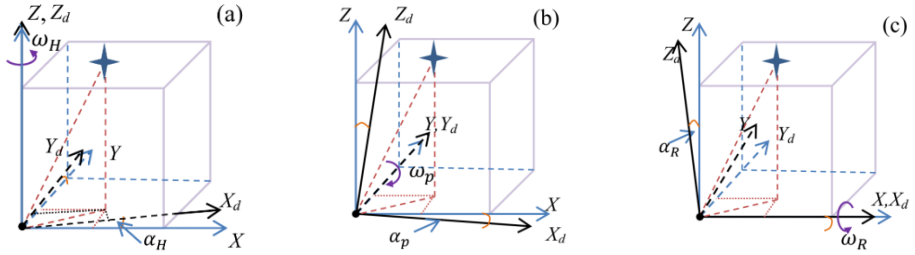

Figure 2 The schematic diagram of motion attitude decouple (a) yawing (b) pitching (c) rolling

Firstly, the submarine rotate α_H around the OZ axis with an angular velocity ω_H. Secondly, the submarine rotate α_R around the OX axis with an angular velocity ω_R. Finally, rotate α_P around the OY axis with an angular velocity ω_P. These coordinate transformations could be written as following matrixes.

$$\begin{bmatrix} X_d \\ Y_d \\ Z_d \end{bmatrix} = T_H T_R T_P \begin{bmatrix} X \\ Y \\ Z \end{bmatrix} = \begin{bmatrix} \cos\alpha_H\cos\alpha_P & \cos\alpha_P\sin\alpha_H & \sin\alpha_p \\ -\sin\alpha_H\cos\alpha_R - \cos\alpha_H\sin\alpha_R\sin\alpha_P & \cos\alpha_H\cos\alpha_R - \sin\alpha_R\sin\alpha_H\sin\alpha_P & \cos\alpha_P\sin\alpha_R \\ -\cos\alpha_H\sin\alpha_P\sin\alpha_R + \sin\alpha_R\sin\alpha_H & -\cos\alpha_H\sin\alpha_R - \sin\alpha_H\sin\alpha_P\cos\alpha_R & \cos\alpha_P\cos\alpha_R \end{bmatrix} \begin{bmatrix} X \\ Y \\ Z \end{bmatrix} \tag{1}$$

By equation 1, the optical axis polar coordinates $(A_\mathrm{d}, E_\mathrm{d})$ can be obtained by $(X_\mathrm{d}, Y_\mathrm{d}, Z_\mathrm{d})$ in submarine coordinate system with

$$\begin{cases} A_d = \arctan(Z_d/X_d) \\ E_d = \arcsin(Y_d/L) \end{cases} \tag{2}$$

Combine the equation 1 and 2, it can obtain:

$$\begin{cases} A_d = arctan\left\{\dfrac{[cosE[cos\alpha_R sin(A-\alpha_H) + sin\alpha_P sin\alpha_R \cos(A-\alpha_H)] - sinE cos\alpha_P sin\alpha_R]}{sinE sin\alpha_P + cosE cos\alpha_P \cos(A-\alpha_H)}\right\} \\ E_d = arcsin\{sin\alpha_P cos\alpha_R \cos(A-\alpha_H) + cos\alpha_P cos\alpha_R sinE - cosE[sin\alpha_R \sin(A-\alpha_H)]\} \end{cases} \tag{3}$$

In photoelectric tracking system, the target is guided into the tracking view by radar or other equipment, and then based on the CCD the servo control system error can be obtained. Meanwhile, by the above equations the rotation angle velocities could be obtained by inertial equipment and navigation algorithms. Then transferring these rotation angle velocities in navigation coordinate to submarine coordinate. The (A_d, E_d) of the target in submarine coordinate could be calculated and guide FSM error compensation.

4. The force character and disturbance solving

In this paper within Δt, the moment evolutions of submarine were only discussed, due to the effect of translation motion for angle tracking error could be neglected. The total pressure difference as well as viscosity moment coefficients is defined as $M_{\mathrm{total}\,p} = 2F_p l/(\rho U_\infty^2 S)$、$M_{total\,v} = 2F_v l/(\rho U_\infty^2 S)$, respectively, where S=0.3613 is the surface area and l=1 is the chord of the submarine.

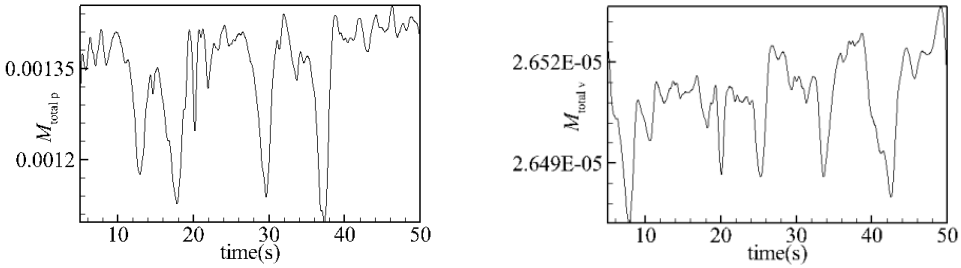

Figure 3 The moment coefficients of submarine (a) pressure gradient force (b) viscous force

As figure 3 shows, the fluctuation of $M_{\mathrm{total\,p}}$ range from 0.0011 to 0.0016, and the $M_{\mathrm{total\,v}}$ range

from 2.646×10^{-5} to 2.654×10^{-5}. The could be seen that $M_{\text{total p}}$ is about 50 times larger than $M_{\text{total v}}$, thus in the following solution the effect of $M_{\text{total v}}$ for submarine could also be ignored. The action effect of force and moment mainly depends on the submarine mass. Moreover, as error compensation device FSM, its reflected light needs to pass a telescope system so there is an optical magnification between the deflection angle of FSM and the light actual output angle. Furthermore, the practical need deflection angle of FSM at each time step of feedback control will also keep a proportional relation with the action effect of the total moment. Here we set k as this proportional coefficient.

$$k = \overline{M_{\text{total p}}} + \overline{M_{\text{total v}}}$$

In reality, if the submarine levitate over the seawater, uncertainly roll would be appears due to the flow moment. In this simulation, the submarine keep 6 ° yaw angle, thus during the solution and analysis procedure, we assume that in x, y, z directions three moments with opposite and equal mean value are present. In the real submarine navigation and control, these opposite moments are usually obtained by propeller and horizontal rudder. The moment disturbances produced by the fluid can be considered as fluctuating around their mean values, in each directions. Comparing with figure 3, the figure 4 shows the time histories of C_{mpx}、C_{mpy}、C_{mpz}, which have subtracted their mean values.

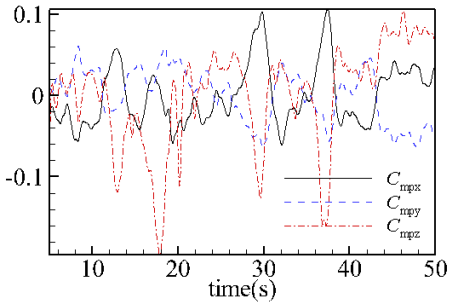

Figure 4 The time histories of disturbance coefficient as well as their mean values

Take the C_{mpx}、C_{mpy}、C_{mpz} in figure 4 into the equation 3, and set the initial azimuth is 0.6, the initial pitch angle is 0.1. These solutions of $A_d$and E_d displayed in figure 5. Figure 5 shows that A_d and E_d fluctuate within 0.5 to 0.65 and -0.05 to 0.15, and the E_d appears larger fluctuation amplitude, while A_d is larger than E_d. Figure 5 also shows that the minimal values of A_d appear at 9s、13s、19s、22s and 38s. In order to deeply analyze the internal mechanism, the characters of flow field structure have mainly been compared and discussed, at these times.

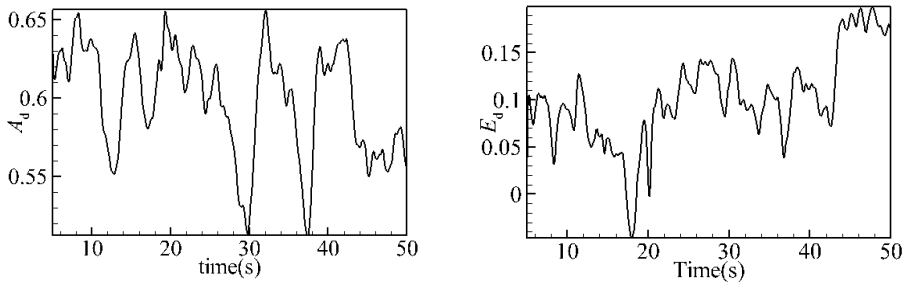

Figure 5 The time histories of A_d and E_d

Figure 6 displays the distributions of λ_2 vortex at 9s, 13s, 19s, 22s and 38s. It could be found that the vortex mainly generates around the submarine's hull, and spreads to the downstream. The λ_2 vortexes are composed by various kinds of small disturbance vortexes, which are of higher frequency characters. Thus, submarine moment fluctuation presents higher frequency and narrow amplitude. The phenomenon could be seen from the time histories of A_d and E_d in figure 5.

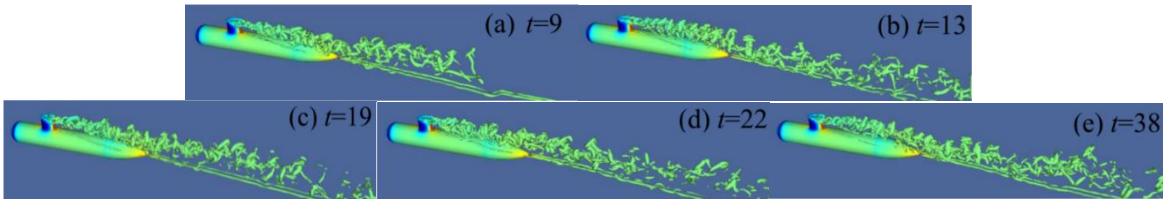

Figure 6 The λ_2 vortex field around the submarine at different time

Figure 6 illustrates the dissipation trail of λ_2 vortexes are of a certain amplitude fluctuation. The origin of this fluctuation is the unbalanced pressure distribution around the rear of the submarine. Due to the large surface of the submarine, the influence of boundary layer for surface pressure difference and viscous force need accumulate and release for a long time, while these phenomena appear certain significant fluctuation and reflect on the trajectory of λ_2 vortexes, as figure 6 shows. This is the key reason for the fluctuation of A_d and E_d curves at 9s, 13s, 19s, 22s and 38s.

5. The analysis of FSM error compensation in the optical tracking system

The closed loop transfer function of this FSM has been tested by collimator, which is written as:

$$G_{\mathrm{FSM}}(s) = \frac{1}{(0.0036\mathrm{s}+1)(2.53^{-6}s^2+0.0022\mathrm{s}+1)}$$

The change of azimuth and pitch angles just reflects the fluid distraction from the submarine and tracking system. However, in order to reveal the influence of both submarine and target $y(t) = 0.2\sin(0.2t+0.2), (5<t<50)$ is added to A_d and E_d.

$$A_{d-\sin}(t) = A_d(t) + y(t), (5<t<50);$$
$$E_{d-\sin}(t) = E_d(t) + y(t), (5<t<50);$$

The superposition curves shown in figure 7.

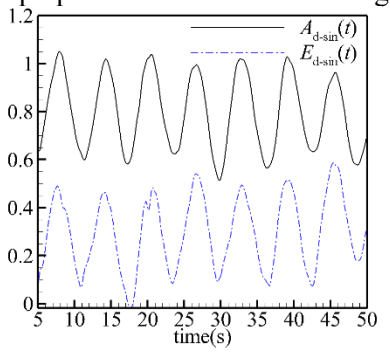

Figure 7 The curves of azimuthal and pitch angles forcomposed by a sinusoidal signal

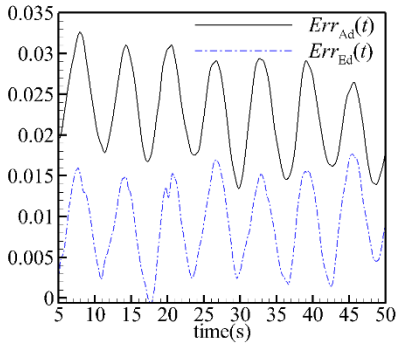

Figure 8 The time histories of angle errors azimuthal and pitch angles

In Matlab Simulink simulation, the $A_{d\text{-}sin}$ and $E_{d\text{-}sin}$ have been inputted to the simulate control system as total disturbance. The PID control parameters are determined through the equal amplitude oscillation method, and the azimuth and pitch angle tracking errors are obtained, shown in figure 8. It could be found that Err_{Ad} and Err_{Ed} fluctuated within 0.014~0.033 and 0~0.017, respectively. And the extreme values of the error appear a character of synchronous changes. Through the flow field analysis, most of the vortexes are of smaller scale and generated from the top of hull. Accordingly, these vortex-induced vibrations generate less fluid dynamics, which caused less significant fluctuation of moment and tracking error. However, the influences of pressure difference force and viscous force on both sides of the submarine produces a significant fluctuation of the dissipation trail consist of small scale vortexes.

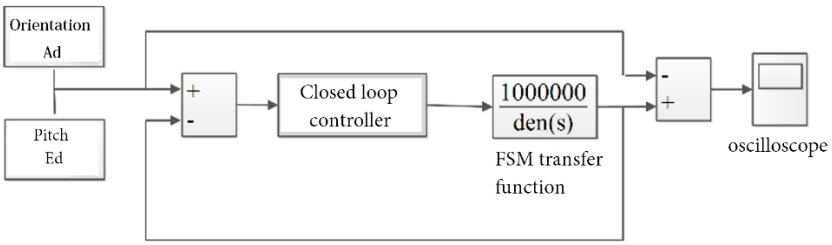

Figure 9 The simulation flow chart by MATLAB

In figure 9 the mean values of azimuthal and pitch angle are $\overline{A_{d-\sin}} = 0.796$, $\overline{E_{d-sin}} = 0.298$. After the error compensation by FSM Matlab simulation both of the error mean values are $\overline{E\mathrm{rr}_{Ad}} \approx 0.0227$, $\overline{E\mathrm{rr}_{Ed}} \approx 0.009$. We can obtain the mean error percent of azimuthal and pitch angle $\overline{\mathrm{Err}_{Ad}}$ and $\overline{\mathrm{Err}_{Ed}}$ to their respective mean values $\overline{A_{d-sin}}$ and $\overline{E_{d-sin}}$, which can be written as:

$$(\overline{E\mathrm{rr}_{Ad}}/\overline{A_{d-sin}}) \times 100\% = 2.85\%$$
$$(\overline{E\mathrm{rr}_{Ed}}/\overline{E_{d-sin}}) \times 100\% = 3.00\%$$

The tracking accuracy for azimuthal angle improved remarkably than the pitch angle, because of the 6° yaw makes the submarine suffer more fluid distribution on azimuth axis.

6. Conclusion

This paper, firstly, based on the basic governing equations of hydromechanics, the influences of pressure and viscous moment on 6° yaw submarine motion tendencies (rolling angle, pitch angle and course angle) have been numerical simulated and analyzed by finite volume method and the structure grid model. Secondly, through the perturbation solution, the three movement trends are transformed into the submarine coordinate system under the photoelectric tracking and aiming system, and the influence of moment on the azimuth angle and the pitch angle is obtained. Finally, construct the closed-loop transfer function of FSM and photoelectric simulation model of control system by MATLAB simulation. And the compensation effects of tracking precision for dynamic target in azimuth and pitching axis by FSM are compared and analyzed, respectively.

Acknowledgements

This research is sponsored by the Chinese National Natural Science Foundation Grant No. 11702139.

References

[1] Chen Z B, Li G N, Liu X Y, et al. The structure form layout and installation design about car-based photonics mast[J]. Journal of Discrete Mathematical Sciences and Cryptography, 2017, 20(1): 231-238.
[2] Hiskett P A, Lamb R A. Underwater optical communications with a single photon-counting system [C]//Proc. SPIE. 2014, 9114: 91140P.
[3] Manshadi M D, Hejranfar K, Farajollahi A H. Effect of vortex generators on hydrodynamic behavior of an underwater axisymmetric hull at high angles of attack[J]. Journal of Visualization, 2017, 2(1):1-21.
[4] Vaz G, Toxopeus S, Holmes S. Calculation of manoeuvring forces on submarines using two viscous-flow solvers[C].Proceedings of the ASME 2010 29th International Conference on Ocean, Offshore and Arctic Engineering, Shanghai, 2010. ASME.
[5] Tian J, Yang W, Peng Z, et al. Application of MEMS accelerometers and gyroscopes in fast steering mirror control systems[J]. Sensors, 2016, 16(4): 440.
[6] Horvat R, Jezernik K, Curkovic M. An event-driven approach to the current control of a BLDC motor using FPGA[J]. IEEE Transactions on Industrial Electronics, 2014, 61(7): 3719-3726.
[7] Popinet S. An accurate adaptive solver for surface-tension-driven interfacial flows. J. Comput Phys, 2009, 228(16): 5838-5866 Popinet S 2009 J. Comput. Phys. 228 5838.

[8] Popinet S, Rickard G. A tree-based solver for adaptive ocean modelling. Ocean Modelling, 2007, 16(3-4): 224-249 Popinet S, Rickard G 2007 Ocean Modelling 2007 16 224.
[9] Liu Z K, Bo Y M, Wang J, et al. Lorentz force filtering and fast steering mirror optical compensation in optical axis stability control for photoelectric mast[J]. Acta Physica Sinica, 2017, 66(8).